STUbL-mediated degradation of the transcription factor MATα2 requires degradation elements that coincide with corepressor binding sites

Christopher M. Hickey and Mark Hochstrasser
Department of Molecular Biophysics and Biochemistry, Yale University, New Haven, CT 06520

ABSTRACT **The yeast transcription factor MATα2 (α2) is a short-lived protein known to be ubiquitylated by two distinct pathways, one involving the ubiquitin-conjugating enzymes (E2s) Ubc6 and Ubc7 and the ubiquitin ligase (E3) Doa10 and the other operating with the E2 Ubc4 and the heterodimeric E3 Slx5/Slx8. Although Slx5/Slx8 is a small ubiquitin-like modifier (SUMO)-targeted ubiquitin ligase (STUbL), it does not require SUMO to target α2 but instead directly recognizes α2. Little is known about the α2 determinants required for its Ubc4- and STUbL-mediated degradation or how these determinants substitute for SUMO in recognition by the STUbL pathway. We describe two distinct degradation elements within α2, both of which are necessary for α2 recognition specifically by the Ubc4 pathway. Slx5/Slx8 can directly ubiquitylate a C-terminal fragment of α2, and mutating one of the degradation elements impairs this ubiquitylation. Surprisingly, both degradation elements identified here overlap specific interaction sites for α2 corepressors: the Mcm1 interaction site in the central α2 linker and the Ssn6 (Cyc8) binding site in the α2 homeodomain. We propose that competitive binding to α2 by the ubiquitylation machinery and α2 cofactors is balanced so that α2 can function in transcription repression yet be short lived enough to allow cell-type switching.**

Monitoring Editor
William P. Tansey
Vanderbilt University

Received: Jun 24, 2015
Revised: Jul 27, 2015
Accepted: Jul 30, 2015

INTRODUCTION

Intracellular protein degradation in eukaryotes is crucial to cellular homeostasis, as it regulates a number of processes and is also responsible for the destruction of abnormal proteins (Varshavsky, 2012). The majority of selective protein degradation in eukaryotic cells is accomplished by the ubiquitin–proteasome system (UPS). Ubiquitin is a highly conserved 76-residue protein that is the prototypical member of the ubiquitin-like proteins (Ubls), which have a common fold and are covalently conjugated to other proteins (Hochstrasser, 2009). The conjugation of ubiquitin to proteins, known as ubiquitylation, requires ATP and involves three enzymes that work sequentially, referred to as the ubiquitin-activating enzyme (E1), ubiquitin-conjugating enzyme (E2), and ubiquitin ligase (E3). E3 enzymes make direct contact with substrate proteins and/or substrate-associated proteins and thus represent the main specificity component of ubiquitylation.

Eukaryotic genomes code for multiple E2s and many E3s (often hundreds), allowing for ubiquitylation of a diverse range of substrate proteins. Ubiquitin is typically conjugated to lysine side chains of substrates. The molecular function of ubiquitin is to enhance affinity of the modified protein for ubiquitin-binding proteins, which can lead to various fates, not all of which involve proteolysis. Modification of a substrate protein by ubiquitin can be in the form of a single ubiquitin (monoubiquitylation) or various ubiquitin polymers (polyubiquitylation), in which one or more of the seven lysine residues or the N-terminal amino group in ubiquitin serve as an acceptor for another ubiquitin. While several forms of polyubiquitin have been discovered in cells, a Lys-48–linked polyubiquitin chain is the most common signal for substrate degradation (Uckelmann and Sixma, 2015).

This article was published online ahead of print in MBoC in Press (http://www.molbiolcell.org/cgi/doi/10.1091/mbc.E15-06-0436) on August 5, 2015.

Address correspondence to: Mark Hochstrasser (mark.hochstrasser@yale.edu).

Abbreviations used: 3HA, triple hemagglutinin and hexahistidine tags; *Deg*, degradation signal; E1, ubiquitin-activating enzyme; E2, ubiquitin-conjugating enzyme; E3, ubiquitin ligase; ER, endoplasmic reticulum; G-6-PDH, glucose-6-phosphate dehydrogenase; MAT, mating type; ORF, open reading frame; SD, synthetic defined; SIM, SUMO-interacting motif; STUbL, SUMO-targeted ubiquitin ligase; SUMO, small ubiquitin-like modifier; Ubl, ubiquitin-like protein; UPS, ubiquitin–proteasome system.

Polyubiquitin chains attached to a protein destined for degradation are recognized by ubiquitin receptors of the proteasome. The proteasome is a 2.6-MDa protein complex that is capable of ubiquitin binding, protein deubiquitylation, substrate unfolding, and substrate translocation into the proteasome core for proteolysis (Tomko and Hochstrasser, 2013). Substrates often have requirements beyond the ubiquitin signal, such as an unstructured region in the substrate capable of initiating binding and unfolding (Inobe and Matouschek, 2014), but the ubiquitylation machinery is the primary component of the UPS that determines whether a protein will be degraded. While many UPS substrates have been described, relatively few have been sufficiently characterized to understand how their propensity to be ubiquitylated and degraded relates to specific properties of the protein.

The *Saccharomyces cerevisiae* cell-type regulator MATα2 (α2) was the first characterized endogenous substrate of the UPS (Hochstrasser and Varshavsky, 1990; Hochstrasser *et al.*, 1991; Rubenstein and Hochstrasser, 2010). The *S. cerevisiae* life cycle includes three stable cell types: two haploid types (a and α) and a nonmating a/α diploid (Haber, 2012). Cell type is determined by the genes of the mating type (*MAT*) locus, which encode proteins that regulate transcriptional programs for mating and cell differentiation. Cells of mating-type α express two proteins, MATα2 and MATα1, from the *MATα* locus. While α2 represses the transcription of the a-specific genes, α1 activates the transcription of α-specific genes. Conversely, cells of mating-type a express a-specific genes, because α2 is absent, and do not express α-specific genes in the absence of α1. Diploid cells repress haploid-specific genes via a heterodimer of α2 and MATa1, the only protein expressed from the *MATa* locus.

An important feature of the yeast life cycle is the ability of homothallic haploid cells to switch mating type, which allows a haploid population that originated as a single mating type to achieve the diploid state. During mating-type switching, the active copy of the *MAT* locus is replaced by information of the opposite mating type from a cryptic (silent) locus in the same chromosome (Haber, 2012). Mating-type switching is rapid, occurring as often as every cell cycle. Together with allelic conversion of the *MAT* locus, rapid mating-type switching requires the elimination of the transcriptional regulators (proteins) of the original cell state (Laney and Hochstrasser, 2003). All three mating-type regulators (α2, α1, and a1) are very short-lived substrates of the UPS in their appropriate haploid type (Chen *et al.*, 1993; Johnson *et al.*, 1998; Nixon *et al.*, 2010). Although similarities have been noted for the UPS-dependent degradation of these three proteins, α2 degradation has been the most extensively studied.

Studies of α2 have also provided a paradigm for transcriptional repression in eukaryotes. The operator regions upstream of a-specific genes contain specific binding sites for α2 and its DNA-binding cofactor Mcm1 (Johnson and Herskowitz, 1985; Keleher *et al.*, 1988, 1989). These binding sites are organized so that two Mcm1 molecules bind in the center, while two α2 molecules bind flanking sequences. Mcm1 and α2 also interact with one another and bind cooperatively to a-specific gene operators (see Figure 8 later in this article). The interaction of α2 with DNA is mediated by its homeodomain, a protein fold found in many eukaryotic transcription factors (Hall and Johnson, 1987; Holland, 2013). Repression by the Mcm1/α2 complex requires the general corepressor complex Tup1/Ssn6 (Cyc8; Komachi *et al.*, 1994; Smith *et al.*, 1995; Malave and Dent, 2006). Structural studies of α2 have yielded a crystal structure of its homeodomain bound to operator DNA (Wolberger *et al.*, 1991) and a structure of an α2 fragment bearing its central linker domain followed by the homeodomain in a ternary complex with DNA and a functional fragment of Mcm1, which binds the linker domain of α2 (Tan and Richmond, 1998).

Turnover of α2 involves two distinct ubiquitylation pathways (Figure 1A; Chen *et al.*, 1993). The best-understood pathway, referred to here as the Doa10 pathway, requires the E2s Ubc6 and Ubc7 and the E3 Doa10, all of which are associated with the endoplasmic reticulum (ER)/nuclear envelope (Swanson *et al.*, 2001). *DOA10* was discovered in a screen for genes that, when mutated, led to the stabilization of protein fusions bearing an N-terminal α2 fragment, known as *Deg1* (for *deg*radation signal *1*). The Doa10 pathway is now known to target many other proteins, including abnormal proteins, for ubiquitylation and degradation (Ravid *et al.*, 2006; Foresti *et al.*, 2013; Ast *et al.*, 2014).

The other major pathway for α2 degradation involves the E2 Ubc4 and the heterodimeric E3 Slx5/Slx8 (Chen *et al.*, 1993; Xie *et al.*, 2010). Notably, cells lacking Slx5/Slx8 do not degrade α2 as slowly as do cells lacking Ubc4, suggesting another Ubc4-dependent E3 or E3s can target α2 for degradation. Therefore we will at times refer to this pathway as the Ubc4 pathway. Slx5/Slx8 localizes to the nucleus, and cells lacking either subunit have phenotypes consistent with roles for Slx5/Slx8 in cell division, genome stability, and DNA repair (Mullen *et al.*, 2001; Zhang *et al.*, 2006; Burgess *et al.*, 2007). Importantly, Slx5/Slx8 binds the Ubl called small ubiquitin-like modifier (SUMO), and SUMO ligation to substrates can recruit Slx5/Slx8 and its functional homologues, collectively known as SUMO-targeted ubiquitin ligases (STUbLs) (Prudden *et al.*, 2007; Sun *et al.*, 2007; Uzunova *et al.*, 2007; Xie *et al.*, 2007). However, the SUMO pathway is not required for Slx5/Slx8-mediated degradation of α2 (Xie *et al.*, 2010). At least one other STUbL, the *Drosophila melanogaster* Degringolade protein, can ubiquitylate both sumoylated and nonsumoylated proteins (Abed *et al.*, 2011).

Proteins destined for degradation by the UPS contain regions that are important for their degradation, referred to here as degradation elements, which in many cases are recognized directly by E3 enzymes or E3 accessory proteins (Ravid and Hochstrasser, 2008). While the term "degradation element" is often used interchangeably with "degradation signal" or "degron," a degron will be defined here as a region of a protein that is both necessary and sufficient to cause degradation. The aforementioned degron known as *Deg1*, which is within the first 67 residues of α2, is sufficient for degradation via the Doa10 pathway (Hochstrasser and Varshavsky, 1990; Swanson *et al.*, 2001). Subsequent mutagenesis of *Deg1* revealed that hydrophobic residues within a predicted amphipathic helix (aa 18–36) are crucial to its degradation (Johnson *et al.*, 1998; Kim *et al.*, 2013). However, mutagenesis of this amphipathic helix (degradation element) in the context of full-length α2 did not stabilize α2 to the level expected for complete lack of Doa10 pathway recognition, suggesting the existence of additional Doa10 degrons within α2 (Johnson *et al.*, 1998). In addition, it remains unclear whether *Deg1* is directly recognized by Doa10. Studies of an artificial degradation sequence known as CL1, which also contains a predicted amphipathic helix and is targeted for degradation by Doa10 (Gilon *et al.*, 1998), suggested that the chaperones Ssa1 (HSP70 family) and Ydj1 (HSP40 family) play an important role in substrate recognition (Metzger *et al.*, 2008).

No degrons or degradation elements within α2 have been reported for the Ubc4 pathway. As previously mentioned, Slx5/Slx8-mediated degradation of α2 does not involve SUMO. Furthermore, Slx5/Slx8 can ubiquitylate α2 in an in vitro assay using purified proteins that do not include SUMO, suggesting that residues within α2 are directly recognized by Slx5/Slx8 (Xie *et al.*, 2010).

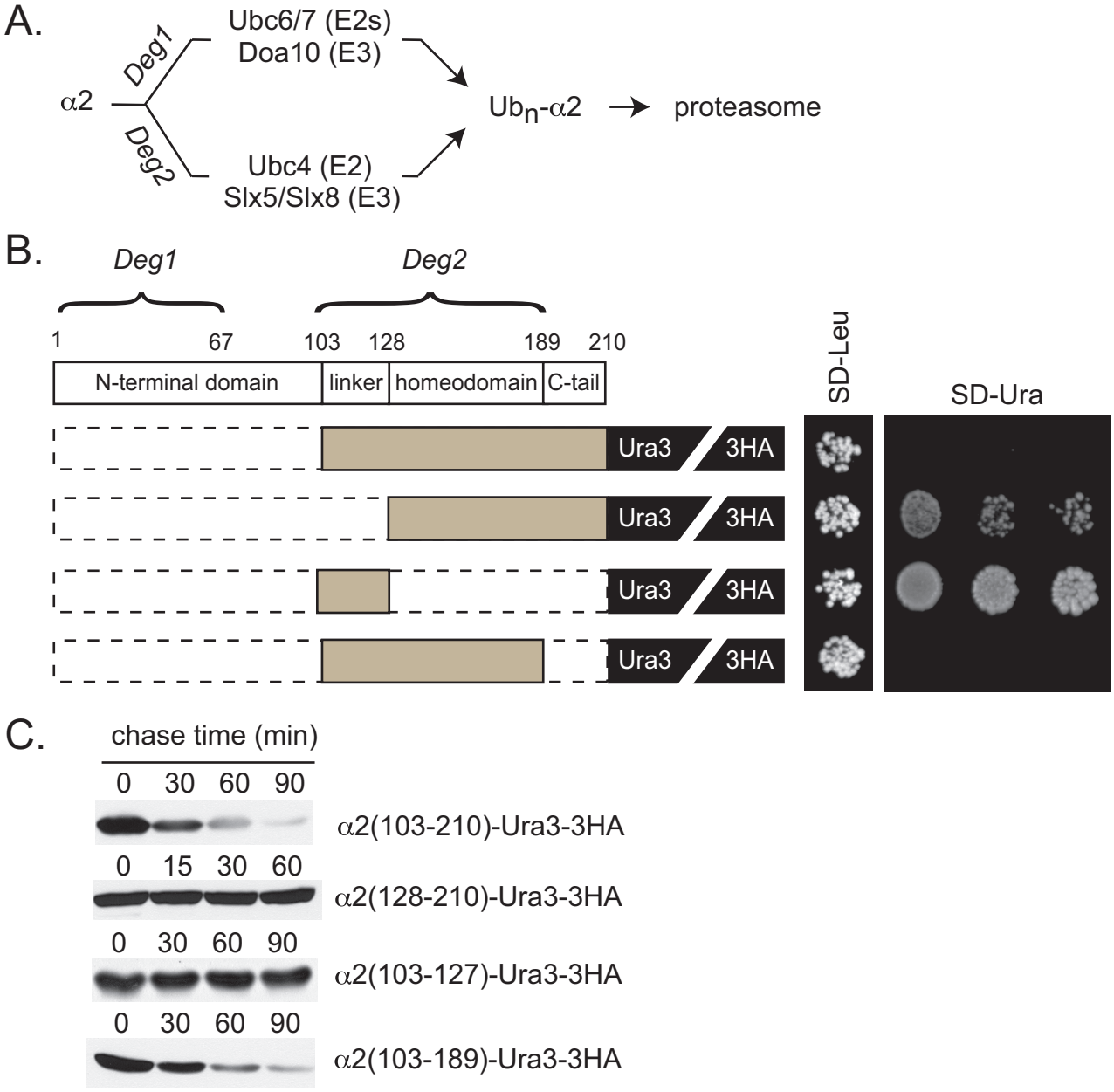

FIGURE 1: Deletion analysis of MATα2 reveals a second degradation signal (*Deg2*) that includes the homeodomain and linker domain. (A) Schematic to summarize α2 degradation in yeast. (B) C-terminal fragments of α2 (gray bars) fused to Ura3-3HA were expressed in a p415MET25 plasmid (*LEU2* backbone). Wild-type yeast cells (MHY501) carrying the indicated constructs were spotted in 10-fold dilution series and tested for growth on solid media lacking leucine (SD-leu) or uracil (SD-ura). Only the most dilute spotted cultures are shown for the plate lacking leucine. Growth on SD-ura is indicative of a stable Ura3-fusion protein. (C) Cycloheximide chase analysis of proteins expressed from p415MET25 plasmids carrying DNA encoding C-terminal fragments of the α2 gene fused to *URA3-3HA*, as described in B. All proteins migrated as expected with no major faster-migrating products detected. Plasmids were transformed into the BY4741 (wild-type) yeast strain.

We now report the identification of a degron in α2 containing two distinct degradation elements for the Ubc4 pathway. One of the degradation elements resides within the homeodomain of α2, overlaps with the interaction site for the cofactor Ssn6, and is directly recognized by Slx5/8. The other newly characterized degradation element is a patch of hydrophobic residues within the central linker domain of α2. Mutation of either degradation element renders α2 immune to the Ubc4 pathway, while maintaining recognition by the Doa10 pathway. The hydrophobic linker element overlaps with the Mcm1 interaction site, but loss of Mcm1 does not stabilize α2. We propose that an unidentified factor cooperates with Slx5/Slx8 to recognize α2 when it is not complexed with Mcm1. Together with previous data that Tup1 and Ssn6 compete with the α2 degradation machinery (Laney *et al.*, 2006), these data show that all the primary degradation elements in α2 coincide with its cofactor binding sites, which may be a more general phenomenon for short-lived regulatory proteins than previously appreciated.

RESULTS

Deletion analysis delimits *Deg2*, a novel degron in α2

MATα2 can be divided into four domains: an N-terminal domain that includes the *Deg1* degron and is largely helical but has not been characterized at the atomic scale, a flexible linker that interacts with Mcm1, a DNA-binding homeodomain, and an unstructured C-terminal tail that participates in heterodimerization with MATa1 in diploid cells (Figure 1B). Because the N-terminal domain of α2 (previously defined as the first 101 residues of α2) was shown to be targeted for degradation mainly by the Doa10 pathway but not the Ubc4 pathway (Johnson *et al.*, 1998), we reasoned that the Ubc4 pathway recognizes an element or elements within one or more of the remaining three domains of α2.

We therefore created a set of constructs that yielded C-terminal α2 fragments fused to the Ura3 protein (also bearing triple hemagglutinin and hexahistidine tags; referred to below as 3HA) and tested the degradation of each protein. Rapid degradation of the Ura3 fusion in a strain with no other source of this uracil biosynthetic enzyme results in poor growth on synthetic defined media lacking uracil (SD-Ura). Based on such growth assays, both the α2 linker and homeodomain (residues 103–189), but not the C-terminal tail, were necessary for the fusion protein to be short lived (Figure 1B). Neither the linker nor the homeodomain alone, however, was sufficient to cause degradation. Each growth assay result was corroborated by cycloheximide chase analysis of protein turnover (Figure 1C). To confirm that the α2(103-189)-Ura3 protein is recognized by the Ubc4-dependent pathway of ubiquitylation, we carried out pulse–chase experiments with this protein. In cells lacking *UBC4*, the reporter protein was indeed stabilized, although not completely, compared with wild-type cells (Supplemental Figure 1). In cells lacking *SLX8*, α2(103-189)-Ura3 was stabilized to a lesser degree than in *ubc4*Δ cells (Supplemental Figure 1), in accord with our previous studies (Xie *et al.*, 2010).

Starting with the α2(103-189)-Ura3 fusion protein, we next tested the degradation of smaller truncations of the linker domain. While secondary structure predictions suggest that the α2 linker (Figure 2A) lacks a stable structure, a crystallographic study of a ternary complex with an α2 C-terminal fragment, Mcm1, and operator DNA revealed an interesting structural dimorphism for the linker (Tan and Richmond, 1998). In the X-ray structure, residues 113–120 of the linker form a β-strand that packs against Mcm1, while residues 121–128 form either a turn-β-strand-turn or an α-helix. The structural dimorphism observed for these latter residues, known as a chameleon sequence, is of unknown physiological consequence. Strikingly, a construct with residues 110–189 of α2 was short lived, whereas a shorter construct with only residues 120–189 of α2 was very stable, as measured by cycloheximide chase analysis (Figure 2A). These data suggest that an element within amino acids 110–120 of the α2 linker is critical for its recognition by the Ubc4 pathway.

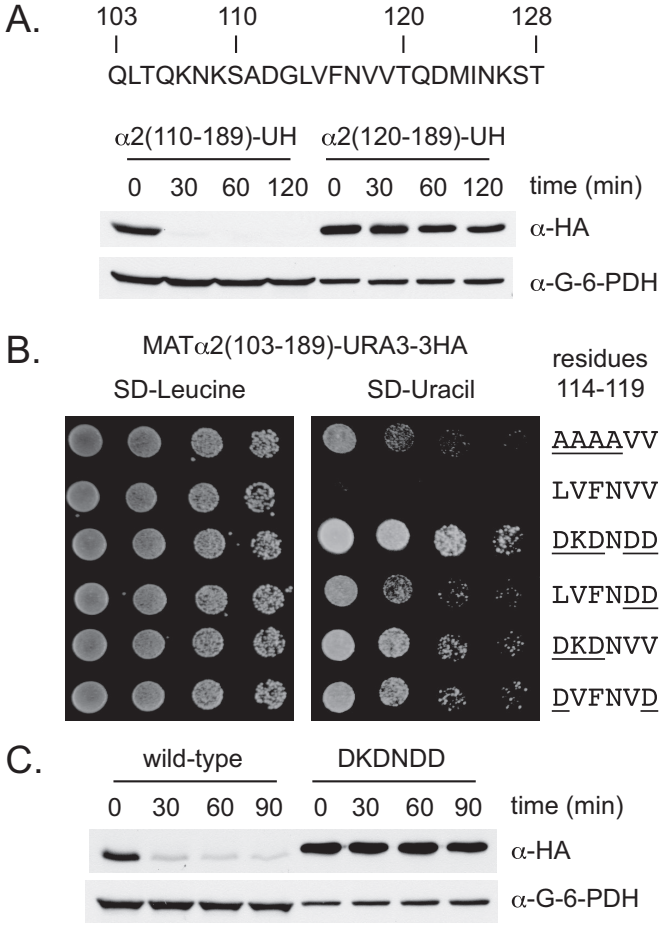

FIGURE 2: A hydrophobic segment within the α2 linker is crucial for *Deg2* function. (A) Cycloheximide chase analysis of the linker truncations α2(110-189)-Ura3-3HA (UH) and α2(120-189)-UH. The amino sequence of the α2 linker, which connects the globular N- and C-terminal domains of α2, is shown above. To avoid a disproportionate signal for α2(120-189)-Ura3-3HA, we loaded fivefold less cell extract compared with that used for α2(110-189)-Ura3-3HA. Immunoblotting for glucose-6-phosphate dehydrogenase (G-6-PDH) was used as a loading control. (B) Constructs based on p415MET25-α2(103-189)-URA3-3HA with the indicated mutations of residues 114–119 were generated, and cells bearing these plasmids were tested for growth on SD-leu or SD-ura after spotting equal cell numbers in sixfold dilution series. (C) Cycloheximide chase analysis of α2(103-189)-Ura3-3HA (wild-type) and α2(103-189;^{114}DKDNDD^{119})-Ura3-3HA. To avoid a disproportionate signal for the ^{114}DKDNDD^{119} version, we loaded fivefold less cell extract compared with the wild-type. The ^{114}DKDNDD^{119} versions of α2 and α2 derivatives consistently run slightly slower than the wild-type during SDS–PAGE. G-6-PDH was used as a loading control. All experiments shown in this figure used MHY501 (wild-type) yeast.

The Mcm1-binding element in the α2 linker is a key *Deg2* component

Because the residues in α2 that make contact with Mcm1 (aa 114–121) are present in the short-lived α2(110-189)-Ura3 protein but are largely absent in the shorter, stable α2(120-189)-Ura3 protein, we chose to focus on the residues within α2 that interact with Mcm1. Previous studies on the interaction between α2 and Mcm1 provided mutants within the Mcm1-binding region of α2 (Mead *et al.*, 1996). One such mutant, in which four consecutive residues (^{114}LVFN^{117}) are mutated to alanine, was incorporated into the α2(103-189)-Ura3 reporter construct and tested by growth assay (Figure 2B). Yeast expressing the α2(103-189, ^{114}AAAA^{117})-Ura3 protein showed a growth rate suggesting significant yet incomplete stabilization of the reporter protein. Working on the hypothesis that hydrophobicity within the linker of α2 is recognized by the UPS machinery, we constructed a mutant in which all five hydrophobic residues of the Mcm1 interaction site were mutated to charged residues. An α2(103-189)-Ura3 mutant in which ^{114}LVFNVV^{119} was mutated to ^{114}DKDNDD^{119} yielded rapid growth on media lacking uracil (Figure 2B), suggesting it is stable. In agreement with the growth assays, cycloheximide chase analysis showed that the ^{114}DKDNDD^{119} mutant fusion protein was very stable (Figure 2C). Mutant derivatives

with fewer than all five hydrophobic residues changed to nonhydrophobic residues yielded slightly less rapid growth compared with the ^{114}DKDNDD^{119} mutant (Figure 2B and Supplemental Figure 2A), suggesting that these hydrophobic residues have a cumulative effect on recognition by the UPS. Also consistent with the idea that general hydrophobicity rather than a specific sequence within the linker of α2 is being recognized by the UPS machinery, mutation of ^{114}AAAA^{117} to ^{114}AAWA^{117} in the α2-Ura3 fusion protein led again to poor growth on media lacking uracil (Supplemental Figure 2B).

Fusion proteins bearing the full chameleon sequence of the α2 linker, but lacking the upstream hydrophobic linker residues, were not short lived (Figure 2), indicating that the chameleon segment of the linker is not sufficient for degron function. To test whether the chameleon sequence is necessary for rapid *Deg2* degradation, we created an α2(103-189; Δ124-127)-Ura3 protein, in which four of the eight residues of the element were deleted (Supplemental Figure 2B). This mutant supported weak growth on SD-Ura medium, suggesting a minor role for the chameleon sequence in *Deg2* degradation.

To analyze the effects of the ^{114}DKDNDD^{119} linker mutation in the context of native α2 protein, we engineered the mutant linker into α2 and quantified its degradation rate by radioactive pulse–chase analysis. The α2-^{114}DKDNDD^{119} protein was approximately twofold more stable than wild-type α2 (Figure 3A), consistent with the degree of stabilization observed for wild-type α2 when the Ubc4 pathway is lost (Chen *et al.*, 1993). Because α2 degradation is only strongly inhibited when both of its major ubiquitylation pathways are eliminated, we tested α2-^{114}DKDNDD^{119} degradation in cells lacking one or both pathways. Strikingly, the mutant α2-^{114}DKDNDD^{119} protein was not further stabilized in cells lacking *UBC4* (Figure 3B). In contrast, α2-^{114}DKDNDD^{119} became much more long lived in cells lacking *UBC6*. Degradation was not further impaired by combining *ubc4*Δ and *ubc6*Δ. These data indicate that the hydrophobic linker element contributes specifically to the Ubc4 pathway.

To determine whether α2 variants with fewer than five substitutions in the linker would behave similarly, we tested the degradation rates of α2 variants with subsets of the residue changes in α2-^{114}DKDNDD^{119}. For this experiment, *ubc6*Δ cells were used to sensitize α2 to loss of targeting by the Ubc4 pathway. As was seen in the context of α2(103-189)-Ura3, the degradation rate of full-length α2 is less defective when only two hydrophobic amino acids are altered to Asp residues compared with the more severe α2-^{114}DKDNDD^{119} mutant (Figure 3C, compare diamonds with squares). Variants of α2 with four or three residues mutated to aspartate in the ^{114}LVFNVV^{119} sequence were also less impaired for degradation relative to α2-^{114}DKDNDD^{119} (Figure 3C, triangles and inverted triangles). Nevertheless, mutation of as few as two hydrophobic residues in the α2 linker results in very significant stabilization of full-length α2 in cells also lacking the Doa10 pathway (Figure 3C, diamonds vs. circles). Taken together, these results show that reducing the hydrophobicity of the Mcm1-interacting site within the α2 linker phenocopies loss of the Ubc4 pathway for α2 degradation.

Because it is no longer sensitive to the Ubc4 pathway, the α2-^{114}DKDNDD^{119} protein is targeted principally by the Doa10 pathway (Figure 3B), much like a protein fused to the *Deg1* degron (Swanson *et al.*, 2001). The ^{114}DKDNDD^{119} linker mutation is thus predicted to sensitize α2 degradation to impairment of the *Deg1* degron. We tested this prediction with a previously characterized single amino acid substitution, F18S, which strongly stabilizes a *Deg1* fusion protein. While the F18S mutation by itself had an extremely modest effect on the turnover rate of α2 (Figure 4A; Johnson *et al.*, 1998), addition of the F18S mutation strongly inhibited degradation of the α2-^{114}DKDNDD^{119} linker mutant (Figure 4B, diamonds). Thus the *Deg1* degron is important for the residual degradation of the α2 protein with a mutated linker.

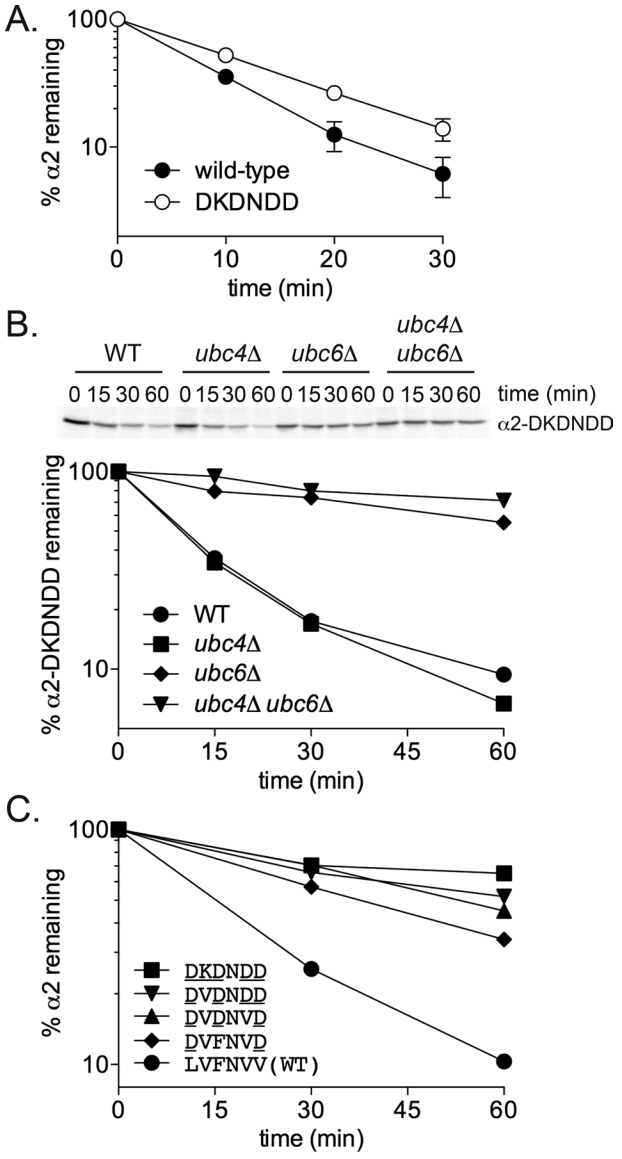

FIGURE 3: An α2 linker mutant phenocopies loss of the Ubc4 pathway for α2 degradation. (A) Quantification of wild-type α2 and α2-^{114}DKDNDD^{119} degradation rates, as determined by radioactive pulse–chase analysis, in cells lacking endogenously expressed α2 (*mat*α*2*Δ; MHY1147). Error bars depict SDs ($n = 3$). (B) Pulse–chase analysis of α2-^{114}DKDNDD^{119} in the following strains: *mat*α*2*Δ ("WT;" MHY1147), *mat*α*2*Δ *ubc4*Δ (MHY1149), *mat*α*2*Δ *ubc6*Δ (MHY1148), and *mat*α*2*Δ *ubc4*Δ *ubc6*Δ (MHY1131), as indicated. The bottom panel is a plot of the pulse–chase data following quantification of band densities. (C) Quantification of degradation rates for the indicated versions of α2, as determined by pulse–chase analysis in MHY1148 cells (*mat*α*2*Δ *ubc6*Δ).

Mcm1 binding is not required for Ubc4-dependent α2 degradation

Given that α2-^{114}DKDNDD^{119} is expected to have reduced interaction with Mcm1, we wished to test whether the α2-Mcm1 interaction

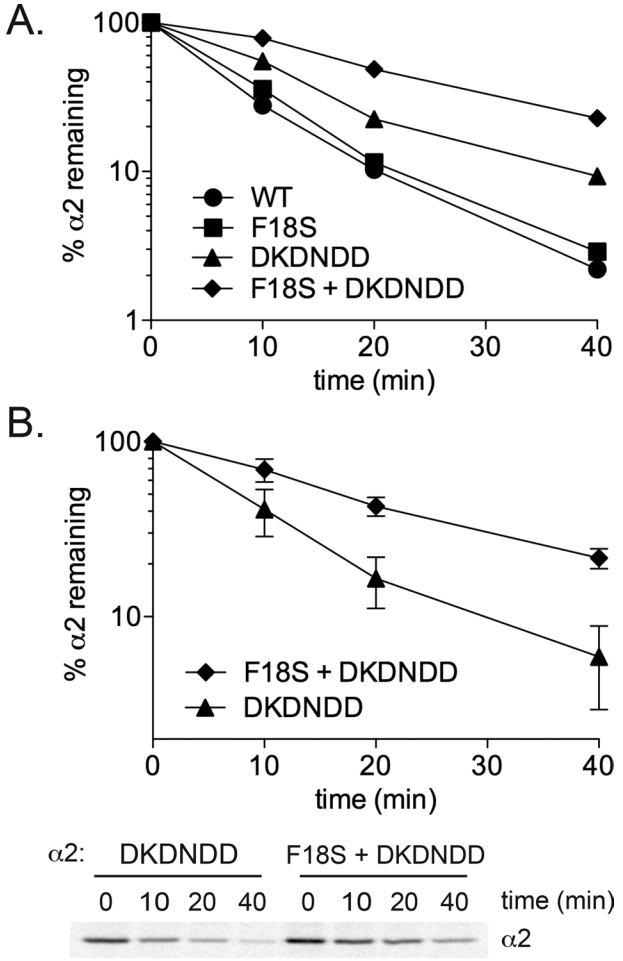

FIGURE 4: The *Deg1* signal acts in a pathway that is genetically distinct from that recognizing the α2 linker element. (A) Quantification of degradation rates for the indicated versions of α2, as determined by pulse–chase analysis, in MHY1147 cells. (B) Quantification of degradation rates for the indicated versions of α2, in triplicate. Error bars depict SDs ($n = 3$). One replicate for each curve is the same data shown in A for the indicated versions of α2. A representative pulse–chase gel is shown below the graph.

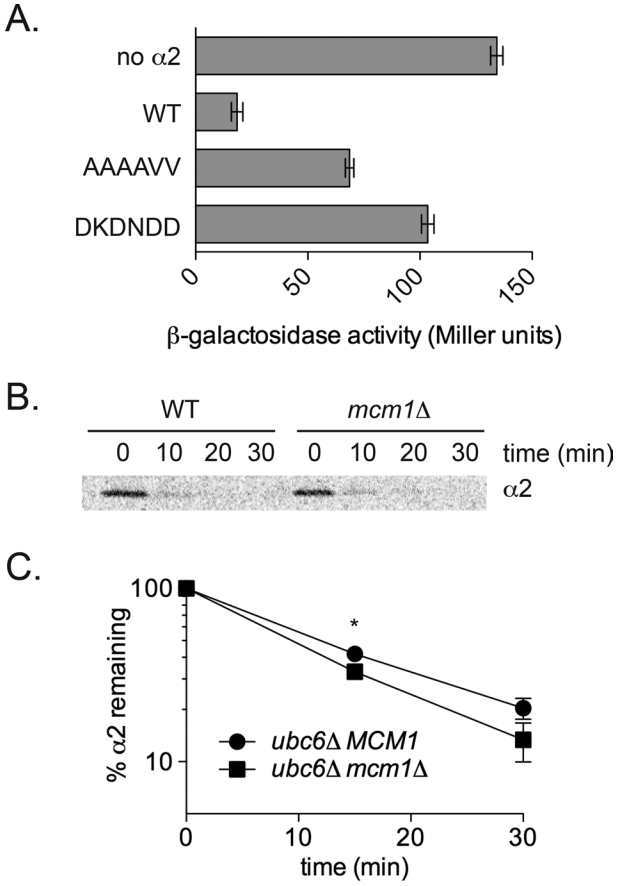

FIGURE 5: Loss of Mcm1 interaction is not responsible for the impaired degradation of the α2 linker mutants. (A) Assay for repression of a-specific gene transcription in MHY481 cells by wild-type α2 or α2 linker variants. LVFNVV (α2 residues 114–119) is the wild-type sequence. Error bars depict SDs ($n = 3$). (B) Pulse–chase analysis of α2 in *mcm1*Δ cells (MHY8661). (C) Quantification of α2 degradation rates, as determined by pulse–chase analysis, in *mcm1*Δ *ubc6*Δ cells (MHY8826). Error bars depict SDs ($n = 3$). *, $p < 0.05$. The *p* value for the 30-min time point is 0.051.

modulates α2 degradation. To verify that the α2-^{114}DKDNDD^{119} protein is indeed deficient in interaction with Mcm1, we measured α2-mediated a-specific gene repression in vivo (Komachi *et al.*, 1994). Haploid yeast lacking an intact *MAT* locus and bearing an integrated a-specific gene operator–controlled *lacZ* gene were transformed with plasmid-borne versions of α2. As predicted, the α2-^{114}DKDNDD^{119} protein was severely deficient in repressing a-specific genes in these cells (Figure 5A). Notably, the α2-^{114}DKDNDD^{119} protein was less functional than α2-^{114}AAAA^{117}, consistent with the expectation that charged residues in place of all five hydrophobic residues is more detrimental to Mcm1 association than the four alanine–substituted mutant.

To determine whether Mcm1 binding has a role in the degradation of the α2 protein, we mutated the α2-binding interface on the Mcm1 protein. A yeast strain that lacked the chromosomal *MCM1* gene was transformed with plasmids expressing either *mcm1-S73R*, a previously described mutant with reduced binding to α2 (Bruhn and Sprague, 1994), or *mcm1-V69E*, which we predicted would also have detrimental effects on α2 interaction based on its impaired interaction with other Mcm1 binding partners (Boros *et al.*, 2003; Darieva *et al.*, 2010; Bastajian *et al.*, 2013). Both *mcm1* mutants degraded α2 at rates similar to those seen in wild-type cells, suggesting that Mcm1 binding is not required for Ubc4-mediated α2 turnover (Supplemental Figure 3A). Consistent with a loss of function, the *mcm1-V69E* and *mcm1-S73R* mutants did not completely complement the growth defect of an *mcm1*Δ strain (Supplemental Figure 3, B and C). Surprisingly, we discovered that cells with no *MCM1* at all were viable (Supplemental Figure 3B). Although *mcm1*Δ cells grew extremely poorly (Supplemental Figure 3, B and C), pulse–chase analysis of α2 degradation revealed that α2 was degraded no more slowly in the absence of Mcm1 (Figure 5B). To provide stronger evidence that the α2-^{114}DKDNDD^{119} protein was not stabilized because of its lack of interaction with Mcm1, we assayed α2 degradation in cells lacking both *MCM1* and *UBC6*, as loss of the Doa10 pathway would exacerbate any weak effects on the Ubc4 pathway. The degradation rate of α2 in *ubc6*Δ *mcm1*Δ cells was no slower than in *ubc6*Δ *MCM1* cells and, in fact, appeared to be slightly faster in the double mutant (Figure 5C).

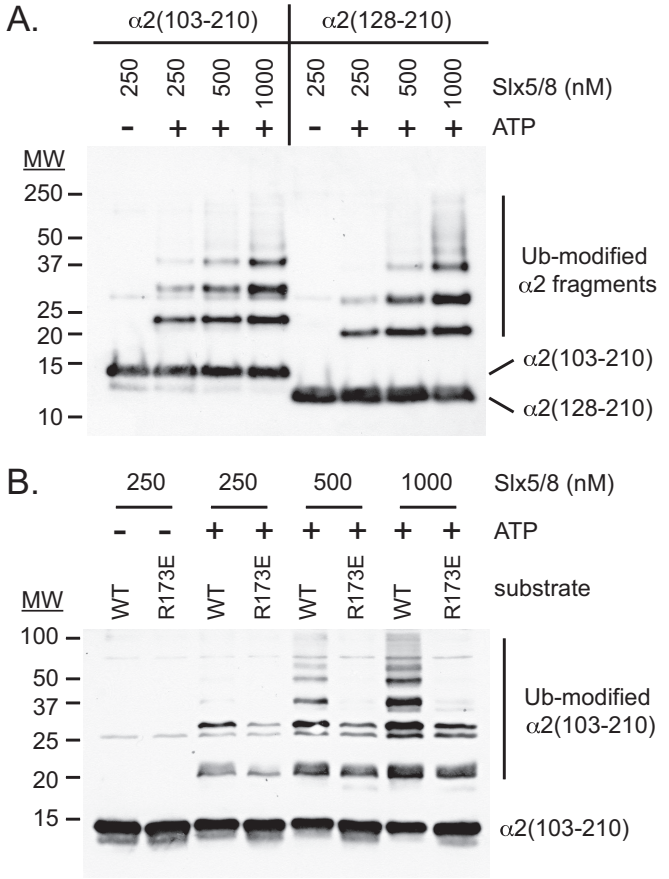

FIGURE 6: Slx5/Slx8 mainly recognizes the homeodomain not the linker of α2. (A) Slx5/Slx8-dependent in vitro ubiquitylation of α2(103-210) and α2(128-210). Reactions contained the indicated concentration of Slx5/Slx8 and a final concentration of 150 mM NaCl and were incubated at 30°C for 30 min. Proteins were separated on a 10% Tris-tricine gel and immunoblotted using anti-α2. (B) Slx5/Slx8-dependent in vitro ubiquitylation of α2(103-210) and α2(103-210; R173E). Reactions contained the indicated concentration of Slx5/Slx8 and a final concentration of 150 mM NaCl and were incubated at 30°C for 30 min. Proteins were separated on a 14% Tris-glycine gel and immunoblotted using anti-α2.

Interaction of α2 with the Slx5/Slx8 ligase in vitro

With the knowledge that α2 is not stabilized when it lacks an interaction with Mcm1, we focused on the idea that the α2-^{114}DKDNDD^{119} protein is stabilized because it fails to interact with another factor. An obvious candidate is the E3 Slx5/Slx8. We employed assays of Slx5/Slx8-α2 interaction and Slx5/Slx8-mediated in vitro ubiquitylation (Xie *et al.*, 2010). However, no differences were observed between α2 and α2-^{114}DKDNDD^{119} in these assays (unpublished data). In a parallel line of investigation, we tested whether C-terminal fragments of α2 could be ubiquitylated in the Slx5/Slx8-dependent in vitro assay. Indeed, a C-terminal fragment of α2 consisting of only the homeodomain and C-terminal tail, α2(128-210)-6His, was efficiently ubiquitylated in an Slx5/Slx8-dependent manner (Figure 6A and Supplemental Figure 4A). However, in vitro ubiquitylation was no more efficient for an α2 fragment bearing the linker domain than one without it (Figure 6A), suggesting that Slx5/Slx8 largely recognizes the homeodomain of α2.

A second Ubc4 pathway degradation element in the α2 repressor

We also screened a previously reported set of α2 homeodomain point mutants for impaired degradation in vivo (Vershon *et al.*, 1995). One mutant, α2-R173A, showed modest stabilization of α2 by pulse–chase (unpublished data). The R173 residue is surface exposed but not directly involved in DNA recognition (Smith and Johnson, 2000). To test whether Slx5/Slx8 has a reduced ability to recognize α2-R173A, we used a C-terminal fragment of α2 bearing this mutation in the in vitro ubiquitylation assay. The α2(103-210; R173A) protein had a modest but reproducible reduction in ubiquitylation in the assay compared with wild-type α2 (Supplemental Figure 4B). To determine whether a less conservative substitution at R173 would have a larger effect on Slx5/Slx8-mediated ubiquitylation of α2, we expressed and purified an α2-R173E fragment and tested its ubiquitylation in the in vitro assay. The α2(103-210; R173E) protein had a striking reduction in ubiquitylation compared with the wild-type version of this protein (Figure 6B). Thus our data show that a degradation element within the homeodomain of α2, which includes the Arg-173 residue, is recognized by Slx5/Slx8.

We next measured the degradation of the full-length α2-R173E protein in wild-type yeast cells and the relevant E2 deletion strains. Like the α2-^{114}DKDNDD^{119} protein, α2-R173E was more stable than wild-type α2, and its degradation was insensitive to Ubc4 pathway perturbation but showed an almost complete dependence on the Doa10 pathway (*ubc6*Δ in Figure 7A). Therefore the α2 homeodomain Arg-173 residue is also a key degradation element specific to the Ubc4 pathway.

Finally, we wished to determine the in vivo ubiquitylation status of α2 and the α2 variants with mutated degradation elements. For this, we employed a construct expressing α2-FLAG-6His that allows tandem affinity purification and (in the second step) the use of stringent, denaturing conditions to achieve highly purified protein preparations. Immunoblot analysis of purified α2-FLAG-6His detected the presence of high-molecular-mass ubiquitylated species, which were absent if cells expressed untagged α2 (Supplemental Figure 5). Like α2, α2-FLAG-6His is stabilized by mutation of either the linker or homeodomain Ubc4 pathway-specific degradation element, as measured by cycloheximide chase in *ubc6*Δ cells (Figure 7B). In contrast to the in vitro ubiquitylation assay results (Figure 6A), the linker is important for ubiquitylation of α2-FLAG-6His in cells (Figure 7C). The greatest reduction in ubiquitylation of α2-FLAG-6His was observed when both the linker and homeodomain were mutated in the same protein, consistent with the degradation rates observed in the cycloheximide chase experiments (Figure 7B). Considered together, these data argue that degradation elements in both the α2 linker and homeodomain contribute to the Ubc4 pathway of α2 ubiquitylation and degradation in vivo and that the homeodomain element contributes directly to Slx5/Slx8 recognition.

DISCUSSION

While the basic organization and multiple biological roles of the UPS are well established (Varshavsky, 2012), many open questions remain regarding substrate selectivity. The yeast genome codes for more than 50 E3 ligases, and humans have as many as 500 E3s. Obtaining a deep understanding of UPS recognition for diverse UPS substrates will help establish general principles for proteolytic specificity, with the hope that one could eventually predict whether a protein will be short lived and which ubiquitylation pathways will target it. Degradation of the classic UPS substrate MATα2 continues to provide important insights into these issues. Importantly, the two principal pathways that target α2 for degradation are conserved from yeast to humans

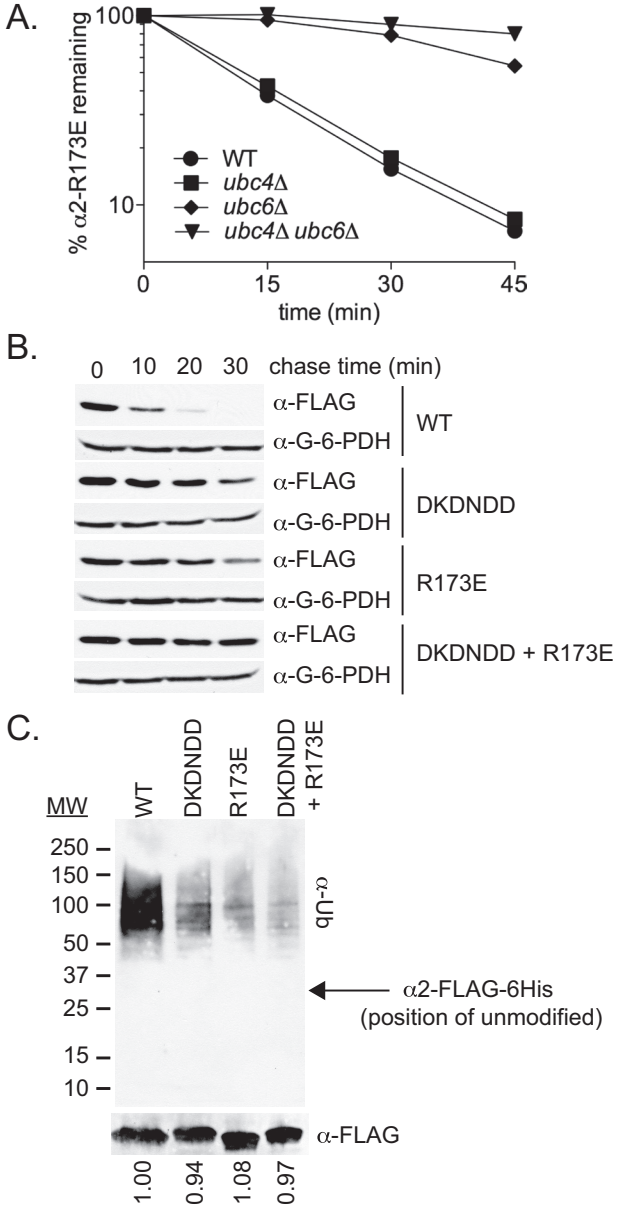

FIGURE 7: (A) The Arg-173 residue of the α2 homeodomain is important for its Ubc4-dependent degradation. Quantification of α2-R173E degradation rates, as determined by pulse–chase analysis, in the following strains (all *matα2Δ*): WT (wild-type; MHY1147), *ubc4Δ* (MHY1149), *ubc6Δ* (MHY1148), and *ubc4Δ ubc6Δ* (MHY1131). (B) Cycloheximide chase analysis of α2-FLAG-6His and indicated variants in *ubc6Δ* (MHY1148) cells. G-6-PDH was used as a loading control. (C) Immunoblot analysis of purified α2-FLAG-6His and indicated variants. Values below the anti-FLAG blot report the levels of the α2-FLAG-6His variants relative to WT α2-FLAG-6His, as quantified using a G:Box system (Syngene).

(Rubenstein and Hochstrasser, 2010). Structural insight into the newly described Ubc4-dependent degradation elements within α2, unlike the Doa10 pathway degron, is possible because the C-terminus of the protein has been characterized at atomic resolution, and our genetically validated in vitro reconstitution of Ubc4-Slx5/Slx8 ubiquitylation of α2 directly suggests potential models for substrate recognition.

A striking result from the current study is that mutation of either of the newly described degradation elements yields an α2 protein that is no longer recognized by the Ubc4 pathway but retains normal recognition by the Doa10 pathway (Figures 3B and 7A). Surprisingly, the α2 linker is dispensable for Ubc4-Slx5/Slx8–mediated ubiquitylation of α2 in vitro (Figure 6A) yet is crucial to the Ubc4 pathway in vivo (Figures 3 and 7). What then is the role of the α2 linker in α2 degradation? We favor the hypothesis that a protein cofactor binds the linker via hydrophobic interactions and cooperates with Slx5/Slx8 to ubiquitylate α2. Linker residues 113–120 of α2 would be exposed in the absence of interaction partners, and the conformation of this segment might be modulated by the downstream chameleon sequence. Molecular chaperone proteins are known to bind exposed hydrophobicity within proteins, and chaperones have been linked to ubiquitylation (Kriegenburg *et al.*, 2012). Potentially, a molecular chaperone could bind both α2 and Slx5/Slx8. Such a factor might be identifiable by addition of yeast proteins to the in vitro ubiquitylation assay that we have developed.

The role of the degradation element within the homeodomain of α2 is more straightforward, as it appears to be a target for Slx5/Slx8 recognition (Figure 6B). Arg-173 is likely only part of the recognition surface, and determining the exact binding interface between Slx5/Slx8 and α2 will require detailed structural analysis. A previous report suggested that Arg-173 is part of a three-residue binding surface for Ssn6, Ser-172 to Ile-174, that is not part of the DNA-binding interface (Smith and Johnson, 2000). Other residues of the homeodomain that are surface exposed might participate in the interaction with Slx5/Slx8 as well (Tan and Richmond, 1998).

Slx5/Slx8 is a relatively large protein complex that may interact with a large surface of α2, especially given that a considerable fraction of Slx5 is expected to be intrinsically disordered (Xie *et al.*, 2007, 2010). The parts of Slx5/Slx8 that associate with α2 are unknown. For sumoylated Slx5/Slx8 substrates, the SUMO-interacting motifs (SIMs) of Slx5 are important for substrate interaction (Xie *et al.*, 2007, 2010). Surprisingly, the SIMs of Slx5 are important for in vivo α2 degradation and in vitro ubiquitylation of α2 despite the fact that SUMO is not involved (Xie *et al.*, 2010). Nevertheless, these SIMs are apparently not essential for α2 binding (Xie *et al.*, 2010). Interestingly, the STUbL from *D. melanogaster* (called Degringolade), which is known to ubiquitylate its substrate Hairy in a SUMO-independent manner, also requires its SIMs for in vitro ubiquitylation of Hairy (Abed *et al.*, 2011). However, the interaction between Degringolade and Hairy involves the Degringolade RING domain rather than its SIMs. Thus, while the requirement for SIMs in the SUMO-independent activity of STUbLs may be conserved, their function in this context remains obscure. Interestingly, genetic data point to a conserved arginine in the Hairy substrate that is important for Degringolade ubiquitylation. This might be analogous to Arg-173 in α2 that is critical for α2 ubiquitylation by Slx5/Slx8 (Figure 6B).

The Doa10 pathway of α2 degradation has been studied extensively, aided in large part by the early identification of the *Deg1* degron (Hochstrasser and Varshavsky, 1990). Our current study reports the identification of another degron within α2, *Deg2* (Figure 1). *Deg2* consists of the linker and homeodomain of α2 and is sufficient to cause the otherwise long-lived protein Ura3 to be degraded in a Ubc4-dependent manner. However, lack of *UBC4* does not completely stabilize *Deg2*-Ura3-3HA (Supplemental Figure 1B), suggesting that *Deg2* can also be recognized by another pathway(s). Whether this is true of full-length α2 or is an artifact of removing the *Deg2* region from its normal context is unclear. However, endogenous α2 is still degraded, albeit slowly, in the absence of both the Doa10 and Ubc4 pathways, leaving open the possibility of an additional α2 degradation pathway(s) (Chen *et al.*, 1993).

Both of the Ubc4-pathway degradation elements described here coincide with interaction sites for α2 cofactors. We previously

showed that overproduction of the corepressors Tup1 and Ssn6 stabilizes α2 (Laney *et al.*, 2006). Tup1 binds to the N-terminal domain of α2 (Komachi *et al.*, 1994), and Tup1 overexpression alone stabilizes *Deg1*-fusion proteins (Laney *et al.*, 2006). Tup1 overexpression only weakly stabilizes full-length α2, as is true for α2 degradation in the absence of only the Doa10 pathway. However, overexpression of both Tup1 and Ssn6, which function as a complex (Varanasi *et al.*, 1996; Malave and Dent, 2006), leads to robust stabilization of α2, similar to that observed when both the Doa10 and Ubc4 pathways are inactive. Ssn6 interacts with the homeodomain of α2, and Arg-173 has been identified as a critical residue for this interaction (Smith *et al.*, 1995; Smith and Johnson, 2000). Thus it appears that Ssn6 and Slx5/Slx8 share an interaction surface on α2 and probably compete for α2 interaction. This idea should eventually be testable with our in vitro ubiquitylation system, but we have not yet succeeded in purifying functional Ssn6 protein.

Our study shows that the interaction site for Mcm1 is also a degradation element for the Ubc4 pathway (Figures 2 and 3). We speculate that an Slx5/Slx8 cofactor competes with Mcm1 for its interaction with α2. In a first attempt to test this idea, we tried to overexpress Mcm1, but this severely inhibited yeast growth (unpublished data). A more direct test of this model would be to determine whether Mcm1 binding inhibits ubiquitylation of α2 in vitro, but our purified assay system does not depend on the α2 linker (Figure 6A), the site of Mcm1 interaction.

Our current and previous findings can be synthesized into a model that accounts for the coincidence of the three major degradation elements in α2—one in *Deg1* for the Doa10 pathway and two for the Ubc4 pathway—with α2 cofactor-binding sites (Figure 8A). When not complexed with cofactors, each of these degradation elements is exposed to the ubiquitylation machinery, allowing for the rapid turnover necessary for mating-type switching. When α2 is bound by its cofactors, such as when it is functioning in a-specific gene repression, it is at least temporarily protected from degradation (Figure 8B). Because α2 and a1 heterodimerize and fully stabilize one another in diploid cells, we speculate that one or both of the Ubc4-pathway degradation elements in α2 is occluded via heterodimerization with a1 (Johnson *et al.*, 1998). By linking susceptibility to ubiquitylation directly to cofactor binding, cells tightly coordinate degradation of the α2 transcription factor with its functional state within the nucleus. We suspect that this is a widespread strategy used to regulate various eukaryotic transcriptional circuits.

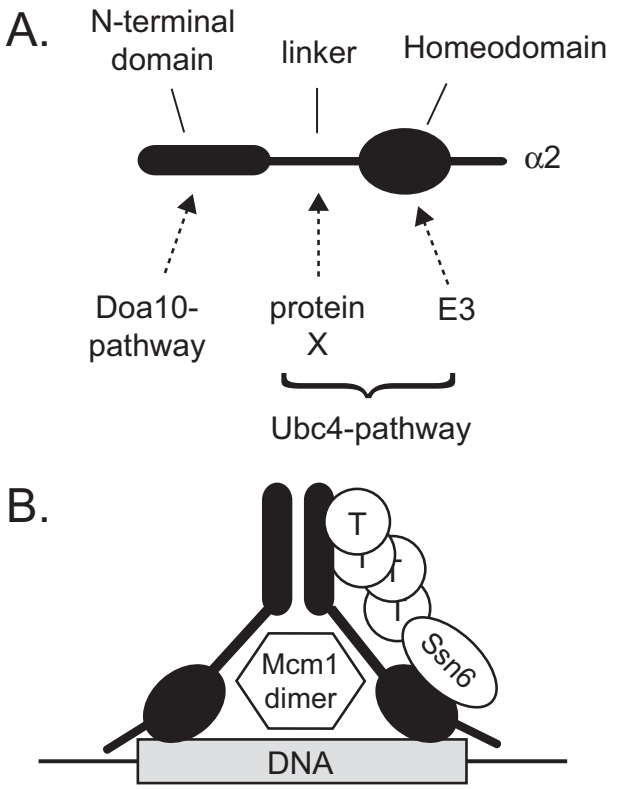

FIGURE 8: Model for α2 degradation. (A) Schematic for the structure of α2, with the regions targeted by each ubiquitylation pathway indicated by dashed lines. (B) Cartoon of how α2 is likely organized on an a-specific gene operator, where it is bound by cofactors that protect it from degradation. Circles labeled "T" represent Tup1. Although Tup1 and Ssn6 are shown binding only one of the α2 subunits in the α2 dimer, this level of detail is unavailable, and these corepressors may bind both copies of α2.

MATERIALS AND METHODS

Strains and plasmids

All yeast strains used in this study are listed in Supplemental Table 1. A diploid yeast strain lacking one copy of the *MCM1* gene was generated by integration at the *MCM1* locus of strain MHY606 of a marker cassette that was amplified by PCR from the pFA6a-kanMX6 plasmid (Longtine *et al.*, 1998). This heterozygous diploid strain was then transformed with the *URA3*-marked plasmid pRS316-MCM1; this was followed by sporulation and tetrad dissection. A spore lacking chromosomal *MCM1* but bearing pRS316-MCM1 was isolated (MHY8591) and then struck on solid media containing 5-fluoroorotic acid (5-FOA). A single colony was isolated, struck again on solid media containing 5-FOA, and a single colony from this plate was struck on solid yeast extract–peptone–dextrose media to isolate the *mcm1*Δ strain (MHY8661). For generation of a *ubc6*Δ *mcm1*Δ strain (MHY8826), a *ubc6*Δ strain (MHY496) was mated to MHY8591, and the resulting diploid was treated as above to isolate a haploid yeast strain that no longer carries the pRS316-MCM1 plasmid.

All plasmids used in this study are listed in Supplemental Table 2. Site-directed mutagenesis was employed to make nucleotide sequence alterations to plasmids (Zheng *et al.*, 2004). Plasmid p415MET25-α2(103-210)-URA3-3HA-6His and the α2(128-210) version of the plasmid were generated by PCR amplification of the respective α2 fusion protein–coding sequences from pJM130-α2-URA3-3HA (Xie *et al.*, 2010) and insertion of the resulting PCR fragments into the *Spe*I and *Hin*dIII sites of p415MET25 (Mumberg *et al.*, 1994). Reporter plasmids encoding α2 fragments not ending with residue 210 were generated by cloning PCR-amplified DNA for the desired α2 fragments into the *Spe*I and *Hin*dIII sites after the *MET25* promoter in a p415MET25-URA3-3HA-6His intermediary vector. For generation of the pRS314-MATα2 plasmid, DNA for the α2 gene plus 584 base pairs upstream and 242 base pairs downstream was PCR amplified from plasmid pJM130 (Mead *et al.*, 1996) and cloned into the *Not*I and *Sal*I sites of pRS314 (Sikorski and Hieter, 1989). Plasmid pRS316-MCM1 was generated by cloning DNA for the *MCM1* gene plus 733 base pairs upstream and 649 base pairs downstream, which was PCR amplified from genomic DNA, into the *Spe*I and *Xho*I sites of pRS316. Point mutations in *MCM1* were introduced in this backbone. The pRS313-MCM1 and pRS313-*mcm1* mutant plasmids were generated by subcloning from the pRS316-based equivalents. Plasmids used for expression of α2 fragments in *Escherichia coli* were generated by PCR amplifying the α2 fragments from pJM130, with one primer designed to add DNA for a C-terminal 6His tag and stop codon immediately following the

final codon from α2, and cloning into the *Nde*I and *Xho*I sites of pET21a (Novagen, Darmstadt, Germany).

For generation of the p416-α2promoter-α2-FLAG-6His plasmid for yeast expression, a plasmid with the α2 promoter was first generated by PCR amplifying the 584 base pairs upstream of the α2 open reading frame (ORF) from plasmid pJM130 and cloning this fragment into the *Sac*I and *Bam*HI sites of p416MET25-α2-FLAG (Hwang *et al.*, 2010) to replace the *MET25* promoter. The α2-FLAG ORF from p416MET25-FLAG was then PCR amplified and cloned into the *Nde*I and *Xho*I sites of pET21a so that an in-frame 6His tag encoded by pET21a follows the FLAG tag. A fragment encoding α2-FLAG-6His was then PCR amplified from pET21a-α2-FLAG-6His using a primer designed to remove the *Xho*I site between the FLAG and 6His sequences and to create an *Xho*I site after the DNA coding for the 6His tag. This fragment was then cloned into the *Bam*HI and *Xho*I sites of p416-α2promoter-α2-FLAG to make p416-α2promoter-α2-FLAG-6His.

Yeast protein degradation assays

Pulse–chase experiments were carried out as previously described (Chen *et al.*, 1993). Cell growth for all pulse–chase experiments using p314-MATα2–based plasmids used minimal media lacking tryptophan supplemented with casamino acids (BD, Sparks, MD). [^{35}S]-labeled proteins were immunoprecipitated using a polyclonal antibody against α2 and separated by SDS–PAGE, and the dried gels were exposed to a phosphoimager screen; this was followed by imaging on a STORM 860 (GE, Marlborough, MA) and analysis using ImageQuant 5.2 software (GE).

For cycloheximide chase experiments, yeast carrying the indicated plasmids were grown to logarithmic phase, and cycloheximide was added to a final concentration of 0.25 mg/ml to halt protein synthesis. A culture aliquot was immediately added to ice-cold stop buffer (30 mM sodium azide) for the zero time point, and the chase sample aliquots were then taken at the indicated times from cultures incubated at 30°C and moved to tubes containing stop buffer placed on ice. Cells from each time point were then lysed as described (Kushnirov, 2000), and proteins were analyzed by Western immunoblot analysis using the indicated antibodies.

Assaying a-specific gene repression

Yeast strain MHY481, which lacks the chromosomal *MAT*α locus and bears an integrated *E. coli lacZ* gene under the control of an a-specific gene operator, was transformed with plasmids carrying wild-type or mutated versions of α2. Logarithmically growing cells (1 OD_{600}-ml per reaction) were harvested by centrifugation and resuspended in 0.75 ml of Z buffer (60 mM Na_2HPO_4, 40 mM NaH_2PO_4, 10 mM KCl, 1 mM $MgSO_4$, pH 7.0, plus freshly added 50 mM 2-mercaptoethanol) that had been prewarmed to 30°C. The resuspended cells were then treated with 25 μl of 0.1% SDS and 40 μl of chloroform, vortexed for 30 s, and incubated for 5 min at 30°C to permeabilize the cells. The reactions were started by the addition of 0.150 ml of ortho-nitrophenyl-β-galactoside (4 mg/ml) and stopped after 5 min by the addition of 0.375 ml 1M Na_2CO_3. The tubes were centrifuged at full speed in a tabletop microcentrifuge (Eppendorf 5424), and the absorbance at 420 nm was measured for each supernatant. β-galactosidase activity is expressed as [A_{420} / (A_{600} × volume [in ml] × time [in min])] × 1000.

Recombinant proteins and in vitro ubiquitylation assay

MBP-6His-Slx5 and MBP-6His-Slx8 were expressed and purified from *E. coli* as previously reported (Xie *et al.*, 2007). 6His-Uba1 was expressed and purified from yeast (Carroll and Morgan, 2005). 6His-Ubc4 was purified from *E. coli* as previously described (Ostapenko *et al.*, 2008). For production of recombinant MATα2 fragments with C-terminal 6His tags, they were expressed in Rosetta 2 (DE3) pLysS cells (Novagen) bearing the pET21a-based plasmids described above. Cells were harvested by centrifugation, resuspended in α2 buffer (20 mM HEPES-NaOH, pH 8.0, 500 mM NaCl, 10% glycerol) plus a protease inhibitor mixture (complete tablet minus EDTA; Roche, Indianapolis, IN), and then frozen in liquid nitrogen. The cells were then thawed, DNase (10 μg/ml) was added, and the cells were sonicated on ice three times for 20 s, with 2-min incubations on ice between sonications. The extract was clarified by centrifugation at 30,000 × *g* for 20 min in a F21-8×50y rotor (Fiberlite; Thermo, Rockford, IL), and the proteins were then bound to a TALON resin (Clontech, Mountain View, CA). The resin was washed with α2 buffer supplemented with 10 mM imidazole, and bound protein was eluted in α2 buffer containing 150 mM imidazole. Eluted proteins were buffer exchanged into α2 buffer lacking imidazole using Zeba spin columns (Thermo). In vitro ubiquitylation assays were carried out as previously described (Xie *et al.*, 2010), with minor changes, as noted in the figures and figure legends.

Purification of ubiquitylated α2-FLAG-6His from yeast

Yeast strain MHY1148 (*matα2Δ ubc6Δ*) was transformed with a plasmid expressing α2-FLAG-6His or a mutant version of this protein. Logarithmically growing cells (750 OD_{600}-ml) were incubated in an ice-water bath for 20 min and then harvested by centrifugation at 4°C. Cells were resuspended in 25 ml of ice-cold water, transferred to a 50-ml conical tube, and centrifuged at 4600 × *g* for 3 min at 4°C; the cell pellet was frozen in liquid N_2 and stored at –80°C. The frozen pellet was thawed on ice for 10 min; this was followed by the addition of 3 ml of acid-washed glass beads and 4.5 ml of F buffer (30 mM HEPES, 500 mM NaCl, 1 mM EDTA, 0.2% Triton X-100, 30 mM *N*-ethylmaleimide, and Roche complete, EDTA-free protease inhibitor). This mixture was vortexed seven times for 30 s each with 2-min incubations on ice in between; all procedures were performed at 4°C. The mixture was then centrifuged at 4600 × *g* for 5 min at 4°C. The supernatant was collected and centrifuged in a Type 70.1 Ti rotor at 30,000 × *g* for 30 min at 4°C. The supernatant was collected and protein concentration was measured using the bicinchoninic acid assay (Thermo). An equivalent amount of protein (60 mg) for each sample was added to anti-FLAG beads (100 μl packed resin; Sigma-Aldrich, St. Louis, MO) in a 15-ml conical tube and incubated at 4°C with rotation for 2 h. The mixture was centrifuged at 750 × *g* for 4 min at 4°C, and beads were resuspended in 1 ml of F buffer and transferred to a 1.5-ml microcentrifuge tube. The beads were washed once more with F buffer and four times with H buffer (30 mM HEPES, 500 mM NaCl, 0.2% Triton X-100), with centrifugation at 1500 × *g* for 2 min to pellet the beads. Proteins were eluted by incubating the anti-FLAG beads with 550 μl of H buffer containing 3×FLAG peptide (0.2 mg/ml) for 45 min at 4°C. The beads were removed by centrifugation in Micro Bio-Spin columns (Bio-Rad, Hercules, CA), and the eluate was incubated with HisPur Cobalt resin (25 μl packed resin; Thermo) for 1 h at 4°C. Beads were washed (with 1 ml) twice in H buffer, twice in HU8 buffer (H buffer plus 8 M urea), and once in HU2 buffer (30 mM HEPES, 150 mM NaCl, 0.2% Triton X-100, 2 M urea); and proteins were eluted by boiling beads in 60 μl SDS–PAGE sample buffer. Ubiquitin was detected using a rabbit polyclonal antibody (Dako) and α2-FLAG-6His was detected using an anti-FLAG M2 mouse monoclonal antibody (Sigma-Aldrich).

ACKNOWLEDGMENTS

We thank Jason Berk and Janet Burton for comments on the manuscript. We thank Robert Tomko, Jr. (now at Florida State University), for purified proteins and Andrew Vershon (Rutgers University) for plasmids. This work was supported by National Institute of Health grants GM046904 and GM053756 (to M.H.) and F32GM097794 (to C.M.H).

REFERENCES

Abed M, Barry KC, Kenyagin D, Koltun B, Phippen TM, Delrow JJ, Parkhurst SM, Orian A (2011). Degringolade, a SUMO-targeted ubiquitin ligase, inhibits Hairy/Groucho-mediated repression. EMBO J 30, 1289–1301.

Ast T, Aviram N, Chuartzman SG, Schuldiner M (2014). A cytosolic degradation pathway, prERAD, monitors pre-inserted secretory pathway proteins. J Cell Sci 127, 3017–3023.

Bastajian N, Friesen H, Andrews BJ (2013). Bck2 acts through the MADS box protein Mcm1 to activate cell-cycle-regulated genes in budding yeast. PLoS Genet 9, e1003507.

Boros J, Lim FL, Darieva Z, Pic-Taylor A, Harman R, Morgan BA, Sharrocks AD (2003). Molecular determinants of the cell-cycle regulated Mcm1p-Fkh2p transcription factor complex. Nucleic Acids Res 31, 2279–2288.

Bruhn L, Sprague GF Jr (1994). MCM1 point mutants deficient in expression of alpha-specific genes: residues important for interaction with alpha 1. Mol Cell Biol 14, 2534–2544.

Burgess RC, Rahman S, Lisby M, Rothstein R, Zhao X (2007). The Slx5-Slx8 complex affects sumoylation of DNA repair proteins and negatively regulates recombination. Mol Cell Biol 27, 6153–6162.

Carroll CW, Morgan DO (2005). Enzymology of the anaphase-promoting complex. Methods Enzymol 398, 219–230.

Chen P, Johnson P, Sommer T, Jentsch S, Hochstrasser M (1993). Multiple ubiquitin-conjugating enzymes participate in the in vivo degradation of the yeast MAT alpha 2 repressor. Cell 74, 357–369.

Darieva Z, Clancy A, Bulmer R, Williams E, Pic-Taylor A, Morgan BA, Sharrocks AD (2010). A competitive transcription factor binding mechanism determines the timing of late cell cycle-dependent gene expression. Mol Cell 38, 29–40.

Foresti O, Ruggiano A, Hannibal-Bach HK, Ejsing CS, Carvalho P (2013). Sterol homeostasis requires regulated degradation of squalene monooxygenase by the ubiquitin ligase Doa10/Teb4. Elife 2, e00953.

Gilon T, Chomsky O, Kulka RG (1998). Degradation signals for ubiquitin system proteolysis in *Saccharomyces cerevisiae*. EMBO J 17, 2759–2766.

Haber JE (2012). Mating-type genes and MAT switching in *Saccharomyces cerevisiae*. Genetics 191, 33–64.

Hall MN, Johnson AD (1987). Homeo domain of the yeast repressor alpha 2 is a sequence-specific DNA-binding domain but is not sufficient for repression. Science 237, 1007–1012.

Hochstrasser M (2009). Origin and function of ubiquitin-like proteins. Nature 458, 422–429.

Hochstrasser M, Ellison MJ, Chau V, Varshavsky A (1991). The short-lived MAT alpha 2 transcriptional regulator is ubiquitinated in vivo. Proc Natl Acad Sci USA 88, 4606–4610.

Hochstrasser M, Varshavsky A (1990). In vivo degradation of a transcriptional regulator: the yeast alpha 2 repressor. Cell 61, 697–708.

Holland PW (2013). Evolution of homeobox genes. Wiley Interdiscip Rev Dev Biol 2, 31–45.

Hwang CS, Shemorry A, Varshavsky A (2010). N-terminal acetylation of cellular proteins creates specific degradation signals. Science 327, 973–977.

Inobe T, Matouschek A (2014). Paradigms of protein degradation by the proteasome. Curr Opin Struct Biol 24, 156–164.

Johnson AD, Herskowitz I (1985). A repressor (MAT alpha 2 product) and its operator control expression of a set of cell type specific genes in yeast. Cell 42, 237–247.

Johnson PR, Swanson R, Rakhilina L, Hochstrasser M (1998). Degradation signal masking by heterodimerization of MATα2 and MATa1 blocks their mutual destruction by the ubiquitin-proteasome pathway. Cell 94, 217–227.

Keleher CA, Goutte C, Johnson AD (1988). The yeast cell-type-specific repressor alpha 2 acts cooperatively with a non-cell-type-specific protein. Cell 53, 927–936.

Keleher CA, Passmore S, Johnson AD (1989). Yeast repressor alpha 2 binds to its operator cooperatively with yeast protein Mcm1. Mol Cell Biol 9, 5228–5230.

Kim I, Miller CR, Young DL, Fields S (2013). High-throughput analysis of in vivo protein stability. Mol Cell Proteomics 12, 3370–3378.

Komachi K, Redd MJ, Johnson AD (1994). The WD repeats of Tup1 interact with the homeo domain protein alpha 2. Genes Dev 8, 2857–2867.

Kriegenburg F, Ellgaard L, Hartmann-Petersen R (2012). Molecular chaperones in targeting misfolded proteins for ubiquitin-dependent degradation. FEBS J 279, 532–542.

Kushnirov VV (2000). Rapid and reliable protein extraction from yeast. Yeast 16, 857–860.

Laney JD, Hochstrasser M (2003). Ubiquitin-dependent degradation of the yeast Matα2 repressor enables a switch in developmental state. Genes Dev 17, 2259–2270.

Laney JD, Mobley EF, Hochstrasser M (2006). The short-lived Matα2 transcriptional repressor is protected from degradation in vivo by interactions with its corepressors Tup1 and Ssn6. Mol Cell Biol 26, 371–380.

Longtine MS, McKenzie A III, Demarini DJ, Shah NG, Wach A, Brachat A, Philippsen P, Pringle JR (1998). Additional modules for versatile and economical PCR-based gene deletion and modification in *Saccharomyces cerevisiae*. Yeast 14, 953–961.

Malave TM, Dent SY (2006). Transcriptional repression by Tup1-Ssn6. Biochem Cell Biol 84, 437–443.

Mead J, Zhong H, Acton TB, Vershon AK (1996). The yeast α2 and Mcm1 proteins interact through a region similar to a motif found in homeodomain proteins of higher eukaryotes. Mol Cell Biol 16, 2135–2143.

Metzger MB, Maurer MJ, Dancy BM, Michaelis S (2008). Degradation of a cytosolic protein requires endoplasmic reticulum-associated degradation machinery. J Biol Chem 283, 32302–32316.

Mullen JR, Kaliraman V, Ibrahim SS, Brill SJ (2001). Requirement for three novel protein complexes in the absence of the Sgs1 DNA helicase in *Saccharomyces cerevisiae*. Genetics 157, 103–118.

Mumberg D, Muller R, Funk M (1994). Regulatable promoters of *Saccharomyces cerevisiae*: comparison of transcriptional activity and their use for heterologous expression. Nucleic Acids Res 22, 5767–5768.

Nixon CE, Wilcox AJ, Laney JD (2010). Degradation of the *Saccharomyces cerevisiae* mating-type regulator α1: genetic dissection of *cis*-determinants and *trans*-acting pathways. Genetics 185, 497–511.

Ostapenko D, Burton JL, Wang R, Solomon MJ (2008). Pseudosubstrate inhibition of the anaphase-promoting complex by Acm1: regulation by proteolysis and Cdc28 phosphorylation. Mol Cell Biol 28, 4653–4664.

Prudden J, Pebernard S, Raffa G, Slavin DA, Perry JJ, Tainer JA, McGowan CH, Boddy MN (2007). SUMO-targeted ubiquitin ligases in genome stability. EMBO J 26, 4089–4101.

Ravid T, Hochstrasser M (2008). Diversity of degradation signals in the ubiquitin-proteasome system. Nat Rev Mol Cell Biol 9, 679–690.

Ravid T, Kreft SG, Hochstrasser M (2006). Membrane and soluble substrates of the Doa10 ubiquitin ligase are degraded by distinct pathways. EMBO J 25, 533–543.

Rubenstein EM, Hochstrasser M (2010). Redundancy and variation in the ubiquitin-mediated proteolytic targeting of a transcription factor. Cell Cycle 9, 4282–4285.

Sikorski RS, Hieter P (1989). A system of shuttle vectors and yeast host strains designed for efficient manipulation of DNA in *Saccharomyces cerevisiae*. Genetics 122, 19–27.

Smith RL, Johnson AD (2000). A sequence resembling a peroxisomal targeting sequence directs the interaction between the tetratricopeptide repeats of Ssn6 and the homeodomain of alpha 2. Proc Natl Acad Sci USA 97, 3901–3906.

Smith RL, Redd MJ, Johnson AD (1995). The tetratricopeptide repeats of Ssn6 interact with the homeo domain of alpha 2. Genes Dev 9, 2903–2910.

Sun H, Leverson JD, Hunter T (2007). Conserved function of RNF4 family proteins in eukaryotes: targeting a ubiquitin ligase to SUMOylated proteins. EMBO J 26, 4102–4112.

Swanson R, Locher M, Hochstrasser M (2001). A conserved ubiquitin ligase of the nuclear envelope/endoplasmic reticulum that functions in both ER-associated and Matα2 repressor degradation. Genes Dev 15, 2660–2674.

Tan S, Richmond TJ (1998). Crystal structure of the yeast MATα2/MCM1/DNA ternary complex. Nature 391, 660–666.

Tomko RJ Jr, Hochstrasser M (2013). Molecular architecture and assembly of the eukaryotic proteasome. Annu Rev Biochem 82, 415–445.

Uckelmann M, Sixma TK (2015). Make them, break them, and catch them: studying rare ubiquitin chains. Mol Cell 58, 1–2.

Uzunova K, Gottsche K, Miteva M, Weisshaar SR, Glanemann C, Schnellhardt M, Niessen M, Scheel H, Hofmann K, Johnson ES, *et al*. (2007). Ubiquitin-dependent proteolytic control of SUMO conjugates. J Biol Chem 282, 34167–34175.

Varanasi US, Klis M, Mikesell PB, Trumbly RJ (1996). The Cyc8 (Ssn6)-Tup1 corepressor complex is composed of one Cyc8 and four Tup1 subunits. Mol Cell Biol 16, 6707–6714.

Varshavsky A (2012). The ubiquitin system, an immense realm. Annu Rev Biochem 81, 167–176.

Vershon AK, Jin Y, Johnson AD (1995). A homeo domain protein lacking specific side chains of helix 3 can still bind DNA and direct transcriptional repression. Genes Dev 9, 182–192.

Wolberger C, Vershon AK, Liu B, Johnson AD, Pabo CO (1991). Crystal structure of a MAT alpha 2 homeodomain-operator complex suggests a general model for homeodomain-DNA interactions. Cell 67, 517–528.

Xie Y, Kerscher O, Kroetz MB, McConchie HF, Sung P, Hochstrasser M (2007). The yeast Hex3.Slx8 heterodimer is a ubiquitin ligase stimulated by substrate sumoylation. J Biol Chem 282, 34176–34184.

Xie Y, Rubenstein EM, Matt T, Hochstrasser M (2010). SUMO-independent in vivo activity of a SUMO-targeted ubiquitin ligase toward a short-lived transcription factor. Genes Dev 24, 893–903.

Zhang C, Roberts TM, Yang J, Desai R, Brown GW (2006). Suppression of genomic instability by SLX5 and SLX8 in *Saccharomyces cerevisiae*. DNA Repair (Amst) 5, 336–346.

Zheng L, Baumann U, Reymond JL (2004). An efficient one-step site-directed and site-saturation mutagenesis protocol. Nucleic Acids Res 32, e115.